The Most Massive Objects in the Universe

Daniel E. Holz, T-2; Saul Perlmutter, University of California, Berkeley and LBNL

We predict the most massive object in the universe, finding it to be a cluster of galaxies with total mass M_{200}=3.8×10^{15} $M_\odot$ at z=0.22. We restrict ourselves to self-gravitating bound objects, and base our results on halo mass functions derived from N-body simulations. If an object is found with excessively large mass, or no objects are found near the maximum expected mass, this would be a strong indication of the failure of our standard model for cosmology. Identifying the largest object in the universe is thus a powerful probe, testing non-Gaussianity and the behavior of gravity on large scales.

Our universe has a finite observable volume, and therefore within our universe there is a unique most massive object. This object will be a supercluster of galaxies. Theoretical studies of the growth of structure have now matured, and the mass of the most massive objects can be robustly predicted to the level of a few percent. Furthermore, we are in the midst of a revolution in our ability to conduct volume-limited samples of high-mass clusters, with Sunyaev-Zel'dovich (SZ) and X-ray surveys able to provide complete samples at mass >5×10^{14} $M_\odot$ out to z >1. The masses of the most massive clusters in the universe are therefore a robust prediction of Lamda Cold Dark Matter (ΛCDM) models, as well as a direct observable of our universe.

The cluster mass function is already being utilized as a probe of cosmology, and in particular, of the dark energy equation of state (EOS) [1-3]. What additional value is there in singling out the very tail end of the mass function, representing the most massive clusters in the universe, for special treatment? First, we note that these systems are in many ways the easiest to find, as they are among the largest and brightest objects. They thus avoid many selection effects that might plague lower mass cuts. In addition, these systems constitute a very small sample (ideally, just one compelling candidate), and it is possible to devote significant observational resources to studying them. One might imagine coupled SZ, X-ray, and weak lensing measurements, and thus the masses of these systems will be among the best constrained of any systems. The mass-observable relation for clusters is an essential component in using the cluster mass function to measure properties of the dark energy, and therefore there is a tremendous amount of ongoing work to characterize the masses of these objects [4,5].

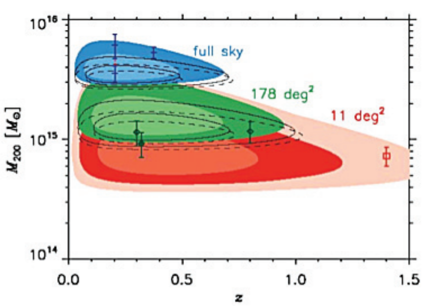

Fig. 1. Contour plot of the most massive object in the universe. Three sets of contours are provided, for three different surveys: full sky, 178deg^2 (corresponding to SPT), and 11deg^2 (corresponding to XMM2235). The shaded contours represent the 1σ and 2σ (and for the 11deg^2 case, 3σ) regions of the most massive halo in a ΛCDM universe. The solid line contours are for the second most massive halo, while the dashed line contours are for the third most massive halo. The (blue) plus signs are Abell 2163 (double point) and Abell 370, the three (green) diamonds are the three most massive clusters in the SPT178deg^2 survey, and the (red) square is XMM2235. Note that the mass values for Abell 2163 span the predicted region, while Abell 370 is slightly high. The SPT masses fit within their respective contours, while XMM2235 is well outside its 2σ contour. All masses are M_{200}: spherical overdensity halos with Δ = 200 (measured with respect to ρ_{matter}). For data measured using different overdensities, we have converted to the M_{200} value, which gives the equivalent probability.

Finally, because we are probing far down the exponential tail of the mass function, these objects offer an unusually powerful constraint. If the most massive object is found to have too large a mass (or especially, as explained below, too small a mass), this single object will provide a strong indication of non-Gaussianity or modified gravity. An excellent example of this is the high-redshift cluster XMMU J2235.3–2557 (hereafter XMM2235), which has been argued to be a few sigma inconsistent with ΛCDM [6,7]. Although much work has focused on using halo statistics as a probe of cosmology, here we focus on using the high-mass tails of precision mass functions to make explicit predictions for current and future observations.

We are interested in determining the mass of the most massive object in our universe. We calculate the expected distribution of masses at the high mass end [8,9], assuming Poisson statistics; the results are shown in Fig. 1. The most massive object in the universe is expected to be found at z =0.22, with a mass M_{200} = 3.8 × 10^{15} $M_\odot$. The marginalized 1σ range in mass is 3.3 × 10^{15} < M_{200} < 4.4 × 10^{15}, while in redshift it is 0.12 < z < 0.36. If the most massive object in the universe falls outside the range 2 × 10^{15} $M_\odot$ < M_{200} < 10^{16} $M_\odot$, we can conclude with high confidence that either the initial conditions are non-Gaussian, or the growth of structure deviates from the predictions of general relativity.

Figure 1 includes contours of the second and third most massive halos in the universe. Going from the most to the second most massive results is a noticeable shift, demonstrating the power of just a few halos to constrain cosmology. As we go further down (e.g., from the second to the third most massive), the contours rapidly converge due to the exponential steepening in expected number at lower mass. Note that the

For more information contact Daniel E. Holz at abc@lanl.gov .

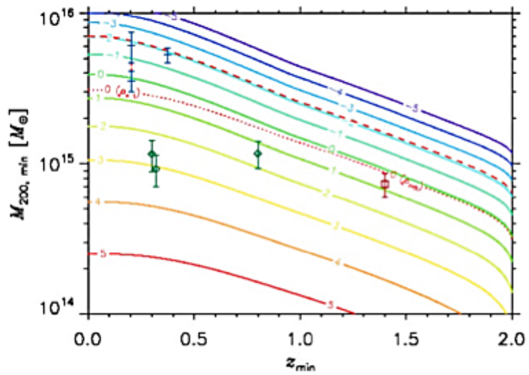

Fig. 2. Expected number of halos at redshift $\geq z_{min}$ with mass $\geq M_{200, min}$, for a full sky survey. Each contour line represents a value of $\log_{10}\langle N \rangle$. For a survey with fraction, *f*, of the full sky, the expected numbers of halos are diminished by the factor *f*. The dashed (red) line shows the result for $\langle N \rangle$ =0.01 using the fit from, based on an FOF halo finder with *b* =0.2. It is virtually indistinguishable from the corresponding SO (Δ = 200) contour. The dotted (red) line represents the $\langle N \rangle$= 1 contour for a Δ =200c mass function, with overdensity compared to ρ_{crit}, instead of the average matter density, ρ_{matter}. Note that this agrees with the fiducial "0" line (Δ =200) at high redshift, as the universe becomes matter-dominated. The data points are the same as in Fig.1.

most massive halo occurs at low redshift. Furthermore, the contours are not centered on the most likely point; there is much larger scatter to high mass, with a sharp lower mass limit, due to the exponential steepening. Note that these likelihoods are not independent, since if the most massive object has an unusually low mass, it is assured that the subsequent few most massive objects will also be unusually low. We have performed Monte-Carlo studies that show that the correlations are weak, however, and the distribution of separations is well approximated by assuming the likelihoods are drawn independently. Figure 1 also shows the contours for the first and second most massive objects from the recent SPT 178deg^2 survey, as well as the contours for the archival XMM-Newton survey that discovered XMM2235.

Figure 2 shows contours of the expected number of halos greater than a given mass, and found beyond a minimum redshift: $\langle N \rangle$ ($> M_{200}$, $> z$).

Perhaps the most compelling candidate for the most massive object in the universe is Abell 2163 at z = 0.203, which has an X-ray mass measurement of $M_{500c} = 3.4 \pm 0.8 \times 10^{15}\, M_\odot$ [10] (where "500c" indicates Δ with respect to $\rho_{\rm crit}$ rather than $\rho_{\rm matter}$). We expect 0.02 (0.002/0.2) clusters with at least this mass and redshift in the entire universe, where the numbers in parentheses are the 1σ lower and upper bounds on $\langle N \rangle$. An alternative, weak lensing measurement of the mass yields a lower value of $M_{500c} = 2.0 \pm 0.3 \times 10^{15}\, M_\odot$, which has expectation 1.4 (0.5/4) (precisely agreeing with predictions). Furthermore, Vikhlinin et al. [11] find an X-ray mass of $M_{500c} = 2.3 \pm 0.07 \times 10^{15}\, M_\odot$, which agrees well with the lensing value. Abell 370 is another compelling candidate, with a weak lensing mass of $M_{\rm vir} = 2.93^{+0.36}_{-0.32} \times 10^{15}\, h^{-1}\, M_\odot$, at z =0.375 [25,26], and an expectation of 0.02 (0.005/0.05). These data points are shown in Figs. 1 and 2, where we have converted the masses to the M_{200} values that give the equivalent probabilities.

Current data argues for further exploration of the highest-mass end of the mass function, both at low and high redshift. It would be particularly difficult, theoretically, to account for excessively massive clusters at $z > 1$, while having agreement at lower redshift (e.g., non-Gaussianity would not suffice). We expect to have dramatically improved complete high-redshift cluster surveys with which to test ΛCDM in the near future, including the full SPT survey (2000deg^2), the Dark Energy Survey (5000deg^2), Planck (all-sky), and eventually the Large Synoptic Suvey Telescope (LSST, 20,000deg^2). In particular, Planck is expected to provide a relatively complete, all-sky survey of all massive clusters out to high redshift in the near future. If the results from these cluster surveys disagree with the predictions outlined above, the ΛCDM paradigm for the growth of structure will need to be revisited.

Special Thanks

We acknowledge valuable discussions with Mark Bautz, Joanne Cohn, Bill Holzapfel, Adam Mantz, Herman Marshall, Elena Pierpaoli, Paul Schechter, Jeremy Tinker, Risa Wechsler, Martin White, and especially Jerry Jungman and Michael Warren.

[1] Holder, G., et al., *Astrophys J Lett* **560,** L111; arXiv:astro-ph/0105396 (2001).
[2] Haiman, Z., et al., *Astrophys J* **553,** 545; arXiv:astro-ph/0002336 (2001).
[3] Cohn, J.D. and M. White, *Mon Not R Astron Soc* **385,** 2025; 0706.0208 (2008).
[4] Kravtsov, A.V., et al., *Astrophys J* **650,** 128; arXiv:astro-ph/0603205 (2006).
[5] Rudd, D.H., et al., *Astrophys J* **672,** 19; arXiv:astro-ph/0703741 (2008).
[6] Jee, M.J., et al., *Astrophys J* **704,** 672; 0908.3897 (2009).
[7] Jimenez, R. and L. Verde, *Phys Rev D* **80,** 127302; 0909.0403 (2009).
[8] Warren, M.S., et al., *Astrophys J* **646,** 881; ArXiv:astro-ph/0506395 (2006).
[9] Tinker, J., et al., *Astrophys J* **688,** 709; 0803.2706 (2008).
[10] Mantz, A., et al., ArXiv e-prints, 0909.3099 (2009).
[11] Vikhlinin, A., et al., *Astrophys J* **692,** 1033; 0805.2207 (2009).

Funding Acknowledgments

LANL Laboratory Directed Research and Development - Exploratory Research